Published in final edited form as:

Mol Cancer Ther. 2019 June ; 18(6): 1045–1056. doi:10.1158/1535-7163.MCT-18-0146.

Inhibition of Ubiquitin-specific protease 14 suppresses cell proliferation and synergizes with chemotherapeutic agents in neuroblastoma

Yang Yu[1,2], **Yanling Zhao**[2], **Yihui Fan**[2], **Zhenghu Chen**[1], **Hui Li**[2], **Jiaxiong Lu**[2], **Kevin Guo**[2], **Sarah E. Woodfield**[1], **Sanjeev A. Vasudevan**[1], **Jianhua Yang**[2], and **Jed G. Nuchtern**[1,2]

[1]Division of Pediatric Surgery, Texas Children's Hospital Department of Surgery, Michael E. DeBakey Department of Surgery, Dan L. Duncan Cancer Center, Baylor College of Medicine, Houston, TX 77030, USA

[2]Texas Children's Cancer Center, Department of Pediatrics, Dan L. Duncan Cancer Center, Baylor College of Medicine, Houston, TX 77030, USA

Abstract

Neuroblastoma (NB) is the most common extracranial malignant solid tumor in children, and drug resistance is a major reason for poor outcomes. Elevated proteasome activity plays an important role in NB tumor development and resistance to conventional chemotherapy. Ubiquitin-specific protease 14 (USP14), one of three deubiquitinases associated with the regulatory subunit of the proteasome, is emerging as a potential therapeutic target in multiple tumor types. However, the role of USP14 in NB is yet to be elucidated. We found that USP14 inhibition in NB via knockdown or a specific inhibitor such as b-AP15 suppressed cell proliferation by inducing cell apoptosis. Furthermore, b-AP15 significantly inhibited NB tumor growth in NGP and SH-SY5Y xenograft mouse models. For combination treatment, b-AP15 plus conventional chemotherapeutic agents such as doxorubicin or VP-16 resulted in synergistic anti-tumor effects on NB. Our study demonstrates that USP14 is required for cell viability and is a novel therapeutic target in NB. Moreover, USP14 inhibition may add value in combination therapy due to its powerful synergistic effects in treating NB.

Keywords

neuroblastoma; ubiquitin-specific protease 14; b-AP15; chemotherapy; synergy

Introduction

Neuroblastoma (NB) is the most common extracranial solid tumor in children and accounts for 8–10% of all childhood tumors (1). Clinically, there are three distinct patterns of disease. Approximately half of children with NB have either localized or locoregional tumors that are

Corresponding authors: Dr. Jed G Nuchtern, 6701 Fannin St., Suite 1210, Houston, TX 77030, United States; phone: +1-832-822-3135; fax: +1-832-825-3141; nuchtern@bcm.edu, Dr. Jianhua Yang, 6701 Fannin St., Suite 1210, Houston, TX 77030, United States; phone: +1-832-824-4572; fax: +1-832-825-1206; jianhuay@bcm.edu.

The authors declare no conflicts of interest.

usually not aggressive and can be treated with surgery and/or moderate doses of adjuvant chemotherapy. The remaining patients have metastatic NB that is difficult to cure, even with intensive, multimodal therapy. Although several molecular and cytogenetic determinants of NB prognosis, such as MYCN amplification (2), ploidy (3), and deletion or loss of heterozygosity of chromosome 1p36 (4), have been identified, the molecular mechanisms associated with these prognostic markers are still not clear. Patients with high risk NB are currently treated with dose-intensive chemotherapy, one or two cycles of myeloablative chemotherapy with peripheral blood stem cell rescue, surgery, radiotherapy, or biologic therapy with retinoids. Although most patients achieve clinical remission, the vast majority of this group will relapse during the first three years off therapy (5). Therefore, identification and functional analysis of novel molecular targets in NB may lead to new options to treat this devastating disease in children.

Dysregulation of the ubiquitin-proteasome system (UPS) is a prominent characteristic of cancer cells. Due to higher rates of protein synthesis and UPS-mediated protein degradation to maintain cell homeostasis, tumor cells are more sensitive to proteasome inhibition (6). The ubiquitination of protein substrates is assembled by an enzymatic cascade involving E1 ubiquitin-activating enzymes, E2 ubiquitin-conjugating enzymes, and E3 ubiquitin ligases. However, ubiquitination is controlled by a group of specialized enzymes called deubiquitinases (DUBs) that remove the ubiquitin modification from protein substrates (7–9). Over 100 DUBs are encoded in the human genome and are classified into six distinct families based on the structural homologies: the ubiquitin-specific proteases (USPs; 54 members in humans), the ovarian tumor proteases (OTUs; 16 members), the ubiquitin C-terminal hydrolases (UCHs; 4 members), the Josephin family (4 members), the motif interacting with ubiquitin (MIU) that contains the novel DUB family (MINDYs; 4 members), and the Zn-dependent JAB1/MPN/MOV34 metalloprotease DUBs (JAMMs, 16 members) (7–10). Due to their protease activity and their involvement in cancer pathologies, DUBs are emerging as potential targets for pharmacological interference in the ubiquitin regulatory machinery (11–13).

USP14, one member of the ubiquitin-specific proteases DUBs family, is associated with the proteasome complex and inhibits proteolysis by catalyzing protein deubiquitination (14). USP14 preferentially removes Lys48-linked polyubiquitin chains from the distal ends, resulting in the shortening of chains to maintain the stability of protein substrates (15, 16). USP14 depletion has little effect on general cell viability in normal physiologic conditions because of functional redundancy with other DUBs (17). However, USP14 plays an essential role in cell survival during vulnerable conditions such as metabolic stress and neuronal development (18–20). Furthermore, evidence has shown that USP14 acts as an oncoprotein in tumorigenesis and metastasis for many solid tumors including colorectal cancer (21), lung cancer (22), and ovarian cancer (23). Thus, USP14 has been identified as a potential therapeutic target in many malignancies. USP14 inhibition via gene knockdown or small molecules induces cell death in breast cancer (24), acute myeloid leukemia (25), and diffuse large B-cell lymphoma (26). However, the function of USP14 in NB has not been examined.

In this study, we focused on the role of USP14 in NB cell survival. Our data demonstrate that USP14 inhibition induces NB cell apoptosis and suppresses tumor growth. In addition,

the combination of USP14 inhibition and conventional chemotherapeutic agents resulted in synergistic anti-tumor effects on NB cells. These findings suggest that USP14 inhibition may serve not only as a stand-alone therapy but also as an effective adjunct to current chemotherapeutic regimens in treating this aggressive pediatric malignancy.

Materials and Methods:

Cell Culture and USP14 knockdown cells

Human NB cell lines used in this study were IMR-32, SK-N-AS, SH-SY5Y (the American Type Culture Collection, ATCC), SK-N-BE2 (Children's Oncology Group, COG), NGP (Deutsche Sammlung von Mikroorganismen und Zellkulturen GmbH, DSMZ), and LAN-6 (a gift from Dr. Robert Seeger). Human embryonic kidney cell lines, HEK293T, HEK293, and human bone marrow stromal cell line HS-5 were also from ATCC. All cell lines were obtained between 2005 and 2017, and authenticated via short tandem repeat (STR) analysis in MD Anderson Cancer Center. *Mycoplasma* testing was performed by LookOut® Mycoplasma PCR Detection Kit (MP0035, Sigma-Aldrich). All NB cell lines were grown in RPMI1640 medium containing 20% heat inactivated fetal bovine serum (Invitrogen), 100 units/ml Penicillin, and 100 μg/ml Streptomycin (Invitrogen). HEK293T, HEK293, and HS-5 cells were grown in DMEM with 10% fetal bovine serum. LAN-6 and SK-N-BE2 were established from NB patients at the time of disease progression after intensive multiagent chemotherapy (27, 28). They are resistant to multiple chemotherapeutic agents including Doxorubicin and VP-16.

For USP14 knockdown in NB cells, all lines were transduced with two independent lentivirus vectors (TRCN0000007425 and TRCN0000007428) specific for *USP14* (Sigma-Aldrich) using standard protocol. Briefly, HEK293T cells were seeded in the 10-cm dish with a concentration of 2.5×10^6 for lentivirus generation. After 24 hours, 6 μg TRC, 2 μg psPAX2 (#12260, Addgene), and 2 μg pMD2.G (#12259, Addgene) plasmids were transfected into cells using lipofectamine 2000 (Life Technologies). The supernatant containing lentivirus was collected 48 hours later. Then, NB cells were transduced with the lentivirus and selected with puromycin (Sigma-Aldrich) (0.5 μg/ml) for 3 days. The USP14 target sequences are CCCAAGATTCAGCAGTCAGAT and CGCAGAGTTGAAATAATGGAA.

Small molecule inhibitors

b-AP15 (#S4920), Doxorubicin (#S1208), and VP-16 (#S1225) were purchased from Selleckchem. b-AP15 and VP-16 were dissolved in DMSO, and Doxorubicin was dissolved in double-distilled water (ddH_2O). Stock solutions were stored at −20°C.

Cell proliferation assays

To determine the effect of USP14 knockdown on NB cell proliferation, 2.0×10^4 cells with control and USP14 knockdown were seeded in each well of a 96-well plate and incubated at 37°C for different time periods. Then cell morphologies were observed and captured using an optical microscope followed by Cell Counting Kit-8 (CCK-8) (Dojindo Molecular Technologies) to measure cell viability. The IC50 value of single agents was calculated

using CompuSyn software based on the data from the cell viability assay (ComboSyn. Inc. Paramus. NJ2007).

To determine the effect of anticancer compounds and USP14 inhibitor on NB cell proliferation, 0.5 to 1.0×10^4 cells were seeded in each well of a 96-well plate and incubated overnight. Compound doses were added to each well individually and cultured for 24 hours. Cell viability was determined using CCK-8 assay.

Clonogenic assay

A total of six NB cell lines were separately seeded into 12-well plates at a concentration of 1×10^4 per well and incubated at 37 °C overnight. Cells were then treated with different dosages (0.375 and 3 μM) of b-AP15 and vehicle controls (DMSO) for 24 hours. After removing the treated medium, all plates were incubated until colonies appeared. For colony staining, the plates were washed two times with ice-cold PBS followed by fixation with ice-cold methanol for 10 minutes. Then, 0.5% crystal violet solution (made with 25% methanol) was added for 10 minutes at room temperature. The plates were rinsed in ddH_2O and dried at room temperature. The stained colonies were photographed and counted via microscope. Each assay was performed in a triplicate.

Colony Formation Assay

The soft agar assay was performed as previously described (29). Briefly, a 0.5% base agarose layer was prepared in a 6-well plate with a volume of 2 ml per well. Then, *USP14* knockdown NB cells were mixed with the 0.3% upper agarose layer at a concentration of 1.0×10^4 per well. Cells were incubated at 37°C and 5% CO_2 for 2 weeks and were stained with 500 μl of 4% formaldehyde and 0.005% crystal violet (C3886, Sigma) for 4 hours. Optical images were captured via microscope and colony numbers were counted. Each assay was performed in a triplicate.

Immunoblotting and antibodies

The immunoblotting was performed as previously described (29). To prepare the whole cell lysates, cells were collected and washed three times with ice-cold phosphate-buffered saline (PBS). Then, cells were lysed by adding RIPA lysis buffer (25 mM HEPES (pH 7.7), 135 mM NaCl, 3 mM EDTA, 1% Triton X-100, 25 mM β-glycerophosphate, 0.5 mM phenylmethylsulfonylfluoride, 1 mM dithiothreitol, 10 μg/ml leupeptin, 1 mM Benzamidine). After centrifuging the lysate at 13,000 g for 15 min at 4°C, protein concentration was measured by Bradford Assay. Cell lysates were resolved with SDS-PAGE and transferred to PVDF membranes. The membranes were probed with appropriate primary antibodies at 4°C overnight and the IgG horseradish peroxidase-conjugated secondary antibodies at room temperature for 1 hour. The proteins were detected using the ECL-Plus Western blotting detection system (Amersham Biosciences) and visualized by autography. Anti-USP14 (A300–920A) was purchased from Bethyl Laboratories. Anti-PARP (9532S), anti-Caspse3 (9662), anti-HSP70 (4872S), anti-HSP40 (4871S), anti-mouse (7076S) and anti-rabbit (7074S) were from Cell Signaling Technology. Anti-β-actin (A2228) was from Sigma-Aldrich. Anti-Ubiquitin (linkage-specific K48) was obtained from Abcam (ab140601).

Cell cycle analysis

USP14 knockdown or control NB cells were harvested after trypsinization and washed with cold PBS buffer. Cold 70% ethanol was used to fix the cells for 30 minutes at 4°C. Then the cells were incubated with PI (50 μg/ml) and RNase (100 μg/ml) solutions for 30 minutes at room temperature in dark room. Flow cytometry was performed to analyze the cell cycle distribution.

Orthotopic xenograft mouse model

Female athymic nude mice (6–8 weeks old) were purchased from Taconic Biosciences. Human NB cell lines NGP and SH-SY5Y with stable expression of luciferase were used to generate human NB orthotopic xenograft mouse models. Briefly, the left kidney of the mouse was exposed with a left flank incision in a sterile manner. 1×10^6 NB cells suspended in 0.1 ml of sterile PBS were surgical injected into the renal capsule. After implantation, tumor growth was monitored weekly by bioluminescent imaging using a Xenogen IVIS Lumina system. Two weeks post-surgery, mice bearing similar bioluminescent signals were randomly divided into two groups treated with either b-AP15 (5 mg/kg) or DMSO daily for two weeks. All mice were euthanized, and tumors were photographed and weighed. All mice were housed in a pathogen-free environment, and all experiments were approved by the Institutional Animal Care and Use Committee of Baylor College of Medicine.

Immunohistochemistry

The xenograft tumors from mice with NGP cells treated with b-AP15 (5 mg/kg) for 2 weeks were preserved in 4% paraformaldehyde for immunohistochemical analysis. Five μm sections of paraffin-embedded (FFPE) tumors were incubated with anti-Ki67 (ab833, abcam) or anti-cleaved Caspase-3 (9664S, cell signaling) for 1 hour at room temperature after blocking with peroxidase. Biotinylated secondary Goat Anti-Rabbit IgG Antibody (21537, Millipore Sigma) and streptavidin-peroxidase (189733, Millipore Sigma) were used to visualize the antigen. Ki67 or Cleaved Caspase-3 positive NGP cells were counted at 20 random high-power fields per xenograft using a light microscope (Nikon).

Drug combination analysis

For drug combination analysis, the method developed by Chou and Talaly was used (30). Dose-response curves and IC50 values for b-AP15, Doxorubicin, and VP-16 in NB cell lines were determined based on the proliferation assay. Equipotent molar ratios between b-AP15 and Doxorubicin or VP-16 were used to treat 96-well plates for 24 hours. Individual treatments of the three drugs were used as controls. The combination index (CI) was assessed by CompuSyn software. $CI < 1$ indicated synergistic interaction, whereas $CI > 1$ was antagonistic, and $CI = 1$ was considered additive effect.

USP14 expression in NB Cohorts

Gene expression of *USP14* was analyzed using R2: Genomics Analysis and Visualization Platform (http://r2.amc.nl). Four publicly available NB cohorts with annotated survival information and gene expression data were analyzed. They are Seqc-498-cohort

(GSE62564), Kocak-cohort (GSE45547), Versteeg-cohort (GSE16476), and Oberthurs-cohort (31) and consist of 498, 476, 88, and 251 NB patient samples, respectively.

Statistical analysis

All *in vitro* experiments were repeated three times, and the representative results were presented. Values were presented as mean ± standard deviation (SD). Statistical significance ($P<0.05$, *; $P<0.01$, **; $P<0.001$, ***) was determined by Student's t-test. Xenograft tumor weights from the various treatment groups were compared using the Kruskal-Wallis test.

Results

USP14 knockdown inhibits NB cell proliferation and induces cell apoptosis

USP14 overexpression has been identified to associate with tumorigenesis in many malignancies (21–23). To determine the role of USP14 in NB, we examined the endogenous USP14 protein levels in a subset of NB cell lines. The immunoblot assay revealed that USP14 was expressed in all NB cell lines tested (Fig. 1A). Next, we suppressed endogenous UPS14 protein with two independent lentivirus short hairpin RNA sequences (sh-RNAs) directed against *USP14* (sh-1 and sh-2) in three MYCN-amplified cell lines: IMR-32, NGP, and SK-N-BE2 (Fig. 1B), and as well in three MYCN-non-amplified cell lines: SH-SY5Y, SK-N-AS, and LAN-6 (Fig. 1C). We found that *USP14* knockdown resulted in inhibition of cell proliferation in all six cell lines (Figs. 1B and 1C). Furthermore, we evaluated the effect of *USP14* knockdown on cell proliferation of two non-tumor cell lines: human bone marrow stromal cell line HS-5 and human embryonic kidney cell line HEK293. No significant changes were detected in these two cell lines with inhibition of *USP14* using sh-RNAs (Supplementary Fig. S1A and S1B).

Previous studies indicated that USP14 regulates cell cycle progression in mouse embryonic fibroblasts (32) and several human adult tumors (22, 33, 34). We examined whether *USP14* knockdown affected the cell cycle distribution in NB cells. Our data show that decreased USP14 expression has little effect on cell cycle progression in NGP and SH-SY5Y cells (Supplementary Fig. S2).

To further understand the molecular mechanisms of the inhibitory effect of *USP14* knockdown on cell proliferation in NB cells, an immunoblotting assay was performed to detect cleaved Caspase 3 and PARP, indicators of apoptosis. Our data show that high levels of Caspase 3 and PARP cleavage were observed in *USP14* knockdown IMR-32, NGP, and SK-N-AS cells and lower levels of Caspase 3 and PARP cleavage were induced in *USP14* knockdown SH-SY5Y, LAN-6, and SK-N-BE2 cells (Figs. 1D and 1E). Taken together, it suggests that USP14 inhibition suppresses cell proliferation at least in part by inducing cell apoptosis.

Besides USP14, UCHL5 and PSMD14 also regulate the function of the eukaryotic 26S proteasome complex by removing the ubiquitin of polyubiquitinated protein substrates (15, 16, 35). We examined the role of these DUBs in NB cell proliferation. We found that UCHL5 knockdown has no effect on NB cell proliferation (Fig. 2A). However, PSMD14 inhibition did result in decreased cell proliferation (Fig. 2B).

USP14 knockdown inhibits cell anchorage-independence growth in NB cells

The capability of anchorage-independent cancer cell growth correlates strongly with tumorigenicity and invasiveness. We next performed the soft agar assay to examine the effect of *USP14* knockdown on cell anchorage-independent growth in NB cell lines. As shown in Figure 2C–2H, *USP14* knockdown led to significant inhibition of anchorage-independent growth of NB cells. Taken together, these results suggest that USP14 plays an important role in NB cell proliferation and tumorigenesis.

USP14 inhibitor b-AP15 suppresses NB cell proliferation

To further examine the inhibitory effect of *USP14* knockdown on NB cell proliferation, a small molecule, b-AP15, which has been reported to specifically act as a USP14 deubiquitinase inhibitor (36), was tested with serial dilutions on a panel of six NB cell lines for 72 hours. A cell viability assay showed that cell proliferation was significantly inhibited in a dose-dependent manner in all tested cell lines (Fig. 3A). The IC_{50} values ranged from 107.8 to 507.0 nM (Fig. 3B). IMR-32 (IC_{50}: 107.8 nM) and LAN-6 (IC_{50}: 127.8 nM) cells were more sensitive while SK-N-BE2 (IC_{50}: 507.0 nM) and SK-N-AS (IC_{50}: 482.5 nM) were more resistant to b-AP15 treatment. These results suggest that the primary mode of action of b-AP15 is independent of MYCN status in NB cells. In addition, b-AP15 induced apoptotic morphological changes of NB cells. As shown in Figure 3C, after treatment of b-AP15 for 72 hours, cytoplasmic shrinkage and cell detachment were observed in many cells. At high dose groups, cytoplasmic vacuolation and cellular fragmentation were clearly seen. A clonogenic assay further verified the cytotoxicity of b-AP15 to tested cells (Supplementary Fig. S3). Significantly fewer clones formed in six cell lines treated with b-AP15 We further evaluated the effect of b-AP15 on cell viability of non-tumor cells, and significantly higher IC50 values in HS-5 and HEK-293 cells than those in NB cells were found (Supplementary Fig. S1C). These results demonstrate that USP14 inhibition suppresses NB cell proliferation.

USP14 inhibition causes accumulation of ubiquitinated proteins and induces unfolded protein response (UPR) in NB

Previous studies showed that blockade of USP14 DUB activity increases intracellular ubiquitinated proteins in many cell types (36, 37). Accumulation of ubiquitinated proteins initiates endoplasmic reticulum (ER) stress resulting in caspase-dependent apoptosis (38, 39). We therefore examined whether UPS14 inhibition causes increased ubiquitinated proteins in NB, and significantly increased ubiquitinated proteins were detected in *USP14* knockdown NGP and SH-SY5Y cells (Fig. 3D). Consistent with this, accumulation of ubiquitinated proteins was also found in these two cells treated with b-AP15 (Fig. 3E). Along with ER stress, ubiquitinated proteins also induce UPR, which increases the expression of heat shock proteins (HSP) (40, 41). Indeed, USP14 inhibition by either sh-RNAs or b-AP15 resulted in induction of HSP70 and HSP40 in both NGP and SH-SY5Y cells (Figs. 3F and 3G).

b-AP15 has synergistic anti-cancer effect with conventional chemotherapeutic agents on NB

Chemotherapy resistance contributes to treatment failure in NB and results in relapse. Therefore, the ability to enhance current chemotherapy efficacy and to overcome established chemoresistance is critical for patients with high-risk NB. We explored whether the USP14 inhibitor b-AP15 could have synergistic anti-cancer effect with Doxorubicin and VP-16 on NB cells. Using the method for synergistic analysis developed by Chou and Talaly (30), b-AP15 was combined with Doxorubicin or VP-16 in seven combinational equipotent ratios based on the IC50 values derived from single treatment of six NB cell lines. Combination indexes (CIs) at the median effective doses 50 (ED50), ED75, and ED90 were derived from tested cell lines using CompuSyn software. As shown in Table 1, we observed synergistic anti-tumor effects at almost all EDs on tested cells. Indeed, there was a strong synergistic anti-cancer effect on Doxorubicin and VP-16 resistant LAN-6 cells. The CI values were 0.25, 0.36, and 0.64 at ED50, 75, and 90, respectively, for the b-AP15 and Doxorubicin combination. The CI values were 0.33, 0.59, and 0.32 at ED50, 75, and 90, respectively, for the b-AP15 and VP-16 combination. Similar results were found in another resistant cell line SK-N-BE2. For deeper molecular mechanistic insights, an immunoblotting assay was used to detect cell apoptosis induced by b-AP15 with Doxorubicin or VP-16 in SK-N-BE2 and LAN-6 cells. We found that b-AP15 treatment can greatly enhance Dox- and VP-16-induced apoptosis since cleaved caspase 3 and PARP levels greatly increased (Supplementary Fig. S4). Our data strongly highlight the potential of USP14 inhibition as an adjuvant therapeutic regimen.

USP14 inhibitor b-AP15 suppresses NB tumor growth *in vivo*

Our *in vitro* data strongly suggest that USP14 is required for NB growth. Next, we examined whether USP14 was also required for NB growth *in vivo*. We utilized an orthotopic NB mouse model produced via surgical injection of NGP and SH-SY5Y cells with luciferase expression into the left renal capsule of nude mice. Two weeks post-surgery, tumor growth was examined with bioluminescent imaging. Mice bearing tumors with similar bioluminescent intensity were randomly divided into two treatment groups: DMSO (control) or b-AP15 (5 mg/kg). Animals were euthanized, and tumors were resected after a daily 2-week treatment. We found that b-AP15 significantly inhibited tumor growth and led to dramatically decreased tumor weights (Figs. 4A and 4B). Then, the NGP xenograft tumors were assessed for tumor cell apoptosis and tumor growth inhibition by immunochemistry staining for cleaved caspase-3 and Ki67. The results showed that b-AP15 significantly inhibited tumor growth and induced apoptosis (Fig. 4C). To further assess the effect of b-AP15 on tumor growth *in vivo*, 4-week post-surgery mice bearing similar tumor signals were treated with b-AP15 (5 mg/kg) for 48 hours. We found that b-AP15 induced cell apoptosis in NB tumors in an immunoblotting assay (Fig. 4D). These results indicate that USP14 inhibition suppresses tumor growth *in vivo* by inducing NB cell apoptosis.

USP14 mRNA level is higher in Stage 4 NB patient samples

USP14 overexpression has been identified and associates with tumorigenesis in many malignancies (21–23). To expand upon these observations and further explore the correlation

between *USP14* mRNA level and survival in NB, we analyzed *USP14* expression in four available public NB cohorts with annotated survival information and gene expression data using R2 genomics analysis and visualization Platform (http://r2.amc.nl). No significant correlation of *USP14* mRNA level with overall and event-free survival was found. The results demonstrated a correlation of *USP14* mRNA level with overall/event-free survival in Seqc-498-cohort of 498 patients (P=0.915/0.493), Kocak-cohort of 476 patients (P =0.843/0.303), Versteeg-cohort of 88 patients (P =0.177/1), and Oberthurs-cohort of 251 patients (P=0.913/0.398) respectively (Fig. 5A and Supplementary Fig. S5A). Moreover, we found that no significant difference of *USP14* mRNA levels was detected between MYCN-amplified NB tumors and MYCN-non-amplified ones (Supplementary Fig. S5B). However, the *USP14* mRNA level was markedly higher in NB tumors of advanced stage 4 disease, compared to that in tumors of lower stages (Figure 5B). Interestingly, we found that *USP14* mRNA levels were lower in stage 4s compared to that in other stages. Therefore, further studies regarding the association between USP14 protein levels and clinical outcome should be performed in NB specimens.

Discussion

Cellular protein homeostasis is a highly regulated characteristic. The ubiquitin–proteasome system (UPS) plays a crucial role in the degradation of short-lived, misfolded, and damaged proteins (42). The UPS has been identified as a key component in the regulation of cancer cell growth and survival. The eukaryotic 26S proteasome complex contains over 50 subunits and can be functionally classified into two functional complexes: the 20S core particle (CP) and the 19S regulatory particle (RP). By removing the ubiquitin of polyubiquitinated protein substrates, three DUBs of the 19S RP, PSMD14, USP14, and UCHL5, regulate the protein degradation function of the 20S CP in mammalian cells (15, 16, 35). The activity of PSMD14, a member of the JAMMs DUBs family, is required for protein substrate degradation by the 20S CP (16). In contrast to PSMD14, USP14 and UCHL5 prevent protein degradation by trimming ubiquitin chains on proteasome-bound substrates (15, 16). Therefore, USP14 and UCHL5 have been suggested to be therapeutic targets in many malignancies (24, 43, 44). To date, the function of USP14 in NB is unknown.

The *USP14* knockdown leads to inhibition of cell proliferation and induction of cell apoptosis in several tumor types including breast cancer (24), non-small cell lung cancer (45), and Ewing sarcoma. Consistent with these results, we found that cell proliferation was dramatically inhibited after *USP14* knockdown in all tested cells. However, *USP14* knockdown has no effect on cell survival in HS-5 and HEK-293 cells. It suggests that targeting DUB activity of USP14 has little effect on cell survival of non-tumor cells in NB, which is similar to the effect of b-AP15 on multiple myeloma (MM) (37). Moreover, the inhibitory effect of *USP14* knockdown is not dependent on *MYCN*-amplification or intact p53 function in NB. As shown in Supplementary Table S1, we used three MYCN-amplified and three MYCN-non-amplified cells. Among these cells, p53 is functional in IMR-32, NGP, SH-SY5Y, and LAN-6, and non-functional in SK-N-AS and SK-N-BE2 cells. In addition, we also found that UCHL5 knockdown has no effect on NB cell proliferation. However, PSMD14 inhibition did result in decreased cell proliferation. Similar to the effects of USP14 inhibition in NB, recent studies also reported that inhibition of PSMD14 DUB

activity by the inhibitor induced apoptosis and overcome bortezomib resistance in multiple myeloma cells (46). It suggests that blockade of PSMD14 could be a potential therapeutic strategy in NB treatment. We will test this hypothesis in future work.

Due to its emerging role in tumors, USP14 has been shown to be a potential therapeutic target. The role of USP14 in UPS regulation is a rate-limiting deubiquitination step prior to protein degradation. By inhibiting the activity of USP14, the levels of ubiquitin conjugated proteins are increased, which triggers proteotoxic stress, eventually inducing cell apoptosis in tumor cells. Recently, many USP14 inhibitors, such as b-AP15 (36), RA-9 (47), and AC17 (48), have been found to inhibit proteasome function by blocking DUB activity. In this study, we provide strong evidence that b-AP15 inhibits NB tumor growth by inducing cell apoptosis *in vitro* and *in vivo* since ubiquitin bound protein levels significantly increase with USP14 inhibition. These findings suggest that USP14 may be a novel target for treatment of NB.

We further demonstrate that USP14 inhibition can be therapeutically exploited to enhance sensitivity and to overcome resistance to conventional chemotherapeutic agents for treating NB. Doxorubicin and VP-16 are often used as intensive chemotherapy for patients with advanced NB (49, 50). However, severe side effects and chemoresistance strictly limit their dosage. Thus, novel enhancers to their anti-tumor activity are highly desirable in the clinical setting. In this study, we provide convincing evidence that the inhibition of USP14 activity greatly enhances Dox- and VP-16-induced cell death in NB cells via experimental treatment on a panel of NB cell lines. Although the efficacy of USP14 inhibitor b-AP15 varied among NB cell lines, the results indicate that b-AP15 can enhance the sensitivity of NB cells to Doxorubicin and VP-16. More importantly, we found a strong synergy of combination treatment in two chemo-resistant cell lines: LAN-6 and SK-N-BE2 (27). These data suggest that the combination of USP14 inhibition and conventional anti-tumor agents is a promising novel therapeutic strategy for NB.

In summary, our study demonstrates that USP14 is a key regulator of cell proliferation in NB and the inhibition of USP14 suppresses tumor growth *in vitro* and *in vivo*. Moreover, USP14 inhibition can overcome chemoresistance and synergize with conventional anti-tumor agents for treating NB. The exact mechanism of synergistic anti-tumor activity of USP14 inhibition is yet to be defined in future work.

Supplementary Material

Refer to Web version on PubMed Central for supplementary material.

ACKNOWLEDGMENTS

We thank Dr. Robert Seeger (Children’s Hospital of Los Angeles) for providing the NB cell lines tested in this paper.

Financial Information: This work was supported by NIH 1R21NS094654 to Dr. J. Yang.

References

1. Castleberry RP. Neuroblastoma. European journal of cancer. 1997;33:1430–7; discussion 7–8. [PubMed: 9337686]
2. Brodeur GM, Seeger RC, Schwab M, Varmus HE, Bishop JM. Amplification of N-myc in untreated human neuroblastomas correlates with advanced disease stage. Science. 1984;224:1121–4. [PubMed: 6719137]
3. Look AT, Hayes FA, Nitschke R, McWilliams NB, Green AA. Cellular DNA content as a predictor of response to chemotherapy in infants with unresectable neuroblastoma. The New England journal of medicine. 1984;311:231–5. [PubMed: 6738617]
4. Fong CT, Dracopoli NC, White PS, Merrill PT, Griffith RC, Housman DE, et al. Loss of heterozygosity for the short arm of chromosome 1 in human neuroblastomas: correlation with N-myc amplification. Proceedings of the National Academy of Sciences of the United States of America. 1989;86:3753–7. [PubMed: 2566996]
5. Maris JM. Recent advances in neuroblastoma. The New England journal of medicine. 2010;362:2202–11. [PubMed: 20558371]
6. Selvaraju K, Mazurkiewicz M, Wang X, Gullbo J, Linder S, D'Arcy P. Inhibition of proteasome deubiquitinase activity: a strategy to overcome resistance to conventional proteasome inhibitors? Drug resistance updates : reviews and commentaries in antimicrobial and anticancer chemotherapy. 2015;21–22:20–9.
7. Clague MJ, Barsukov I, Coulson JM, Liu H, Rigden DJ, Urbe S. Deubiquitylases from genes to organism. Physiological reviews. 2013;93:1289–315. [PubMed: 23899565]
8. Komander D, Clague MJ, Urbe S. Breaking the chains: structure and function of the deubiquitinases. Nature reviews Molecular cell biology. 2009;10:550–63. [PubMed: 19626045]
9. Mevissen TET, Komander D. Mechanisms of Deubiquitinase Specificity and Regulation. Annual review of biochemistry. 2017;86:159–92.
10. Abdul Rehman SA, Kristariyanto YA, Choi SY, Nkosi PJ, Weidlich S, Labib K, et al. MINDY-1 Is a Member of an Evolutionarily Conserved and Structurally Distinct New Family of Deubiquitinating Enzymes. Molecular cell. 2016;63:146–55. [PubMed: 27292798]
11. Daviet L, Colland F. Targeting ubiquitin specific proteases for drug discovery. Biochimie. 2008;90:270–83. [PubMed: 17961905]
12. Allende-Vega N, Saville MK. Targeting the ubiquitin-proteasome system to activate wild-type p53 for cancer therapy. Seminars in cancer biology. 2010;20:29–39. [PubMed: 19897040]
13. Nijman SM, Luna-Vargas MP, Velds A, Brummelkamp TR, Dirac AM, Sixma TK, et al. A genomic and functional inventory of deubiquitinating enzymes. Cell. 2005;123:773–86. [PubMed: 16325574]
14. Leggett DS, Hanna J, Borodovsky A, Crosas B, Schmidt M, Baker RT, et al. Multiple associated proteins regulate proteasome structure and function. Molecular cell. 2002;10:495–507. [PubMed: 12408819]
15. Hanna J, Hathaway NA, Tone Y, Crosas B, Elsasser S, Kirkpatrick DS, et al. Deubiquitinating enzyme Ubp6 functions noncatalytically to delay proteasomal degradation. Cell. 2006;127:99–111. [PubMed: 17018280]
16. Hu M, Li P, Song L, Jeffrey PD, Chenova TA, Wilkinson KD, et al. Structure and mechanisms of the proteasome-associated deubiquitinating enzyme USP14. The EMBO journal. 2005;24:3747–56. [PubMed: 16211010]
17. Jones TD, Buck KW, Plumb RT. The detection of beet western yellows virus and beet mild yellowing virus in crop plants using the polymerase chain reaction. Journal of virological methods. 1991;35:287–96. [PubMed: 1816257]
18. Chen PC, Qin LN, Li XM, Walters BJ, Wilson JA, Mei L, et al. The proteasome-associated deubiquitinating enzyme Usp14 is essential for the maintenance of synaptic ubiquitin levels and the development of neuromuscular junctions. The Journal of neuroscience : the official journal of the Society for Neuroscience. 2009;29:10909–19. [PubMed: 19726649]

19. Chernova TA, Allen KD, Wesoloski LM, Shanks JR, Chernoff YO, Wilkinson KD. Pleiotropic effects of Ubp6 loss on drug sensitivities and yeast prion are due to depletion of the free ubiquitin pool. The Journal of biological chemistry. 2003;278:52102–15. [PubMed: 14559899]
20. Walters BJ, Campbell SL, Chen PC, Taylor AP, Schroeder DG, Dobrunz LE, et al. Differential effects of Usp14 and Uch-L1 on the ubiquitin proteasome system and synaptic activity. Molecular and cellular neurosciences. 2008;39:539–48. [PubMed: 18771733]
21. Shinji S, Naito Z, Ishiwata S, Ishiwata T, Tanaka N, Furukawa K, et al. Ubiquitin-specific protease 14 expression in colorectal cancer is associated with liver and lymph node metastases. Oncology reports. 2006;15:539–43. [PubMed: 16465409]
22. Wu N, Liu C, Bai C, Han YP, Cho WC, Li Q. Over-expression of deubiquitinating enzyme USP14 in lung adenocarcinoma promotes proliferation through the accumulation of beta-catenin. International journal of molecular sciences. 2013;14:10749–60. [PubMed: 23702845]
23. Wang Y, Wang J, Zhong J, Deng Y, Xi Q, He S, et al. Ubiquitin-specific protease 14 (USP14) regulates cellular proliferation and apoptosis in epithelial ovarian cancer. Medical oncology. 2015;32:379. [PubMed: 25429837]
24. Zhu L, Yang S, He S, Qiang F, Cai J, Liu R, et al. Downregulation of ubiquitin-specific protease 14 (USP14) inhibits breast cancer cell proliferation and metastasis, but promotes apoptosis. Journal of molecular histology. 2016;47:69–80. [PubMed: 26712154]
25. Zhao C, Chen X, Zang D, Lan X, Liao S, Yang C, et al. A novel nickel complex works as a proteasomal deubiquitinase inhibitor for cancer therapy. Oncogene. 2016;35:5916–27. [PubMed: 27086925]
26. Delforoush M, Berglund M, Edqvist PH, Sundstrom C, Gullbo J, Enblad G. Expression of possible targets for new proteasome inhibitors in diffuse large B-cell lymphoma. European journal of haematology. 2017;98:52–6. [PubMed: 27301795]
27. Keshelava N, Seeger RC, Groshen S, Reynolds CP. Drug resistance patterns of human neuroblastoma cell lines derived from patients at different phases of therapy. Cancer research. 1998;58:5396–405. [PubMed: 9850071]
28. Keshelava N, Zuo JJ, Chen P, Waidyaratne SN, Luna MC, Gomer CJ, et al. Loss of p53 function confers high-level multidrug resistance in neuroblastoma cell lines. Cancer research. 2001;61:6185–93. [PubMed: 11507071]
29. Fan Y, Ge N, Wang X, Sun W, Mao R, Bu W, et al. Amplification and over-expression of MAP3K3 gene in human breast cancer promotes formation and survival of breast cancer cells. The Journal of pathology. 2014;232:75–86. [PubMed: 24122835]
30. Chou TC, Talaly P. A simple generalized equation for the analysis of multiple inhibitions of Michaelis-Menten kinetic systems. The Journal of biological chemistry. 1977;252:6438–42. [PubMed: 893418]
31. Oberthuer A, Berthold F, Warnat P, Hero B, Kahlert Y, Spitz R, et al. Customized oligonucleotide microarray gene expression-based classification of neuroblastoma patients outperforms current clinical risk stratification. Journal of clinical oncology : official journal of the American Society of Clinical Oncology. 2006;24:5070–8. [PubMed: 17075126]
32. Lee JH, Park S, Yun Y, Choi WH, Kang MJ, Lee MJ. Inactivation of USP14 Perturbs Ubiquitin Homeostasis and Delays the Cell Cycle in Mouse Embryonic Fibroblasts and in Fruit Fly Drosophila. Cellular physiology and biochemistry : international journal of experimental cellular physiology, biochemistry, and pharmacology. 2018;47:67–82.
33. Liao Y, Liu N, Hua X, Cai J, Xia X, Wang X, et al. Proteasome-associated deubiquitinase ubiquitin-specific protease 14 regulates prostate cancer proliferation by deubiquitinating and stabilizing androgen receptor. Cell Death Dis. 2017;8:e2585. [PubMed: 28151478]
34. Huang G, Li L, Zhou W. USP14 activation promotes tumor progression in hepatocellular carcinoma. Oncology reports. 2015;34:2917–24. [PubMed: 26397990]
35. Ambroggio XI, Rees DC, Deshaies RJ. JAMM: a metalloprotease-like zinc site in the proteasome and signalosome. PLoS biology. 2004;2:E2. [PubMed: 14737182]
36. D'Arcy P, Brnjic S, Olofsson MH, Fryknas M, Lindsten K, De Cesare M, et al. Inhibition of proteasome deubiquitinating activity as a new cancer therapy. Nature medicine. 2011;17:1636–40.

37. Tian Z, D'Arcy P, Wang X, Ray A, Tai YT, Hu Y, et al. A novel small molecule inhibitor of deubiquitylating enzyme USP14 and UCHL5 induces apoptosis in multiple myeloma and overcomes bortezomib resistance. Blood. 2014;123:706–16. [PubMed: 24319254]
38. Menendez-Benito V, Verhoef LG, Masucci MG, Dantuma NP. Endoplasmic reticulum stress compromises the ubiquitin-proteasome system. Hum Mol Genet. 2005;14:2787–99. [PubMed: 16103128]
39. Combaret V, Boyault S, Iacono I, Brejon S, Rousseau R, Puisieux A. Effect of bortezomib on human neuroblastoma: analysis of molecular mechanisms involved in cytotoxicity. Mol Cancer. 2008;7:50. [PubMed: 18534018]
40. Hohfeld J, Cyr DM, Patterson C. From the cradle to the grave: molecular chaperones that may choose between folding and degradation. EMBO reports. 2001;2:885–90. [PubMed: 11600451]
41. Fan CY, Lee S, Cyr DM. Mechanisms for regulation of Hsp70 function by Hsp40. Cell Stress Chaperones. 2003;8:309–16. [PubMed: 15115283]
42. Komander D, Rape M. The ubiquitin code. Annual review of biochemistry. 2012;81:203–29.
43. Shukla N, Somwar R, Smith RS, Ambati S, Munoz S, Merchant M, et al. Proteasome Addiction Defined in Ewing Sarcoma Is Effectively Targeted by a Novel Class of 19S Proteasome Inhibitors. Cancer research. 2016;76:4525–34. [PubMed: 27256563]
44. Wang X, Mazurkiewicz M, Hillert EK, Olofsson MH, Pierrou S, Hillertz P, et al. The proteasome deubiquitinase inhibitor VLX1570 shows selectivity for ubiquitin-specific protease-14 and induces apoptosis of multiple myeloma cells. Scientific reports. 2016;6:26979. [PubMed: 27264969]
45. Zhu Y, Zhang C, Gu C, Li Q, Wu N. Function of Deubiquitinating Enzyme USP14 as Oncogene in Different Types of Cancer. Cellular physiology and biochemistry : international journal of experimental cellular physiology, biochemistry, and pharmacology. 2016;38:993–1002.
46. Song Y, Li S, Ray A, Das DS, Qi J, Samur MK, et al. Blockade of deubiquitylating enzyme Rpn11 triggers apoptosis in multiple myeloma cells and overcomes bortezomib resistance. Oncogene. 2017;36:5631–8. [PubMed: 28581522]
47. Brnjic S, Mazurkiewicz M, Fryknas M, Sun C, Zhang X, Larsson R, et al. Induction of tumor cell apoptosis by a proteasome deubiquitinase inhibitor is associated with oxidative stress. Antioxidants & redox signaling. 2014;21:2271–85. [PubMed: 24011031]
48. Zhou B, Zuo Y, Li B, Wang H, Liu H, Wang X, et al. Deubiquitinase inhibition of 19S regulatory particles by 4-arylidene curcumin analog AC17 causes NF-kappaB inhibition and p53 reactivation in human lung cancer cells. Molecular cancer therapeutics. 2013;12:1381–92. [PubMed: 23696216]
49. Neuroblastoma Treatment (PDQ(R)): Patient Version. PDQ Cancer Information Summaries. Bethesda (MD)2002.
50. Maris JM, Hogarty MD, Bagatell R, Cohn SL. Neuroblastoma. Lancet. 2007;369:2106–20. [PubMed: 17586306]

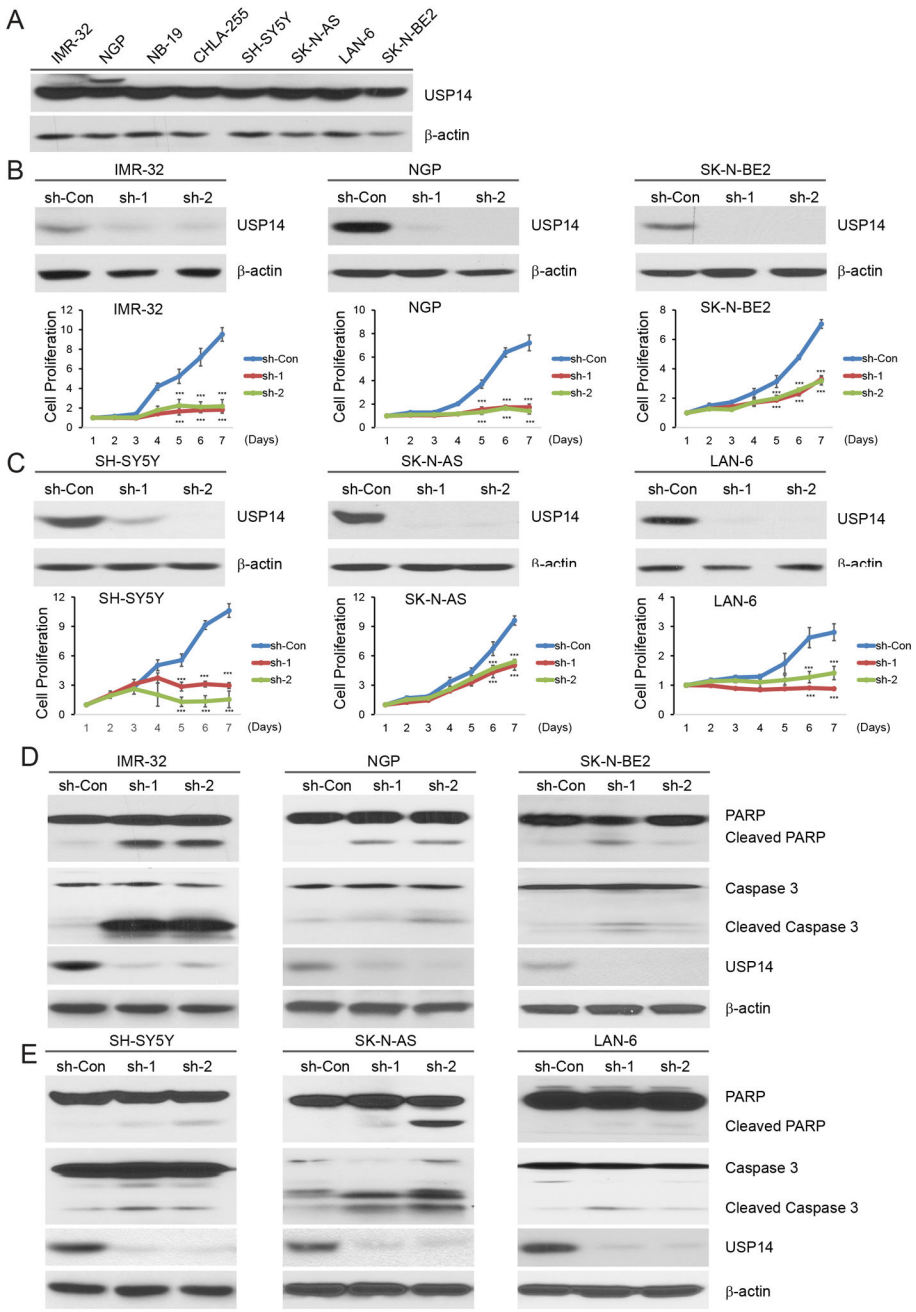

Figure 1: *USP14* knockdown inhibits cell proliferation and induces cell apoptosis in NB.

A. Endogenous expression of USP14 in a panel of NB cell lines including IMR-32, NGP, NB-19, CHLA-255, SH-SY5Y, SK-N-AS, LAN-6, and SK-N-BE2. B, C. Immunoblotting assay showing *USP14* knockdown in IMR-32 (B), NGP (B), SK-N-BE2 (B), SH-SY5Y (C), SK-N-AS (C), and LAN-6 (C) cells by two independent lentivirus shRNAs, sh-1 and sh-2. Cell growth curve assay shows a proliferation defect in six *USP14* knockdown NB cells. The cell counting kit-8 (CCK-8) was used to determine cell viability. Error bars represent SDs of six samples. ***P<0.001. D, E. Six *USP14*-knockdown cells were harvested for the protein immunoblotting assay. PARP and Caspase-3 cleavages were detected by immunoblotting

with the antibodies. β-actin was used as a loading control for whole cell extracts in all samples.

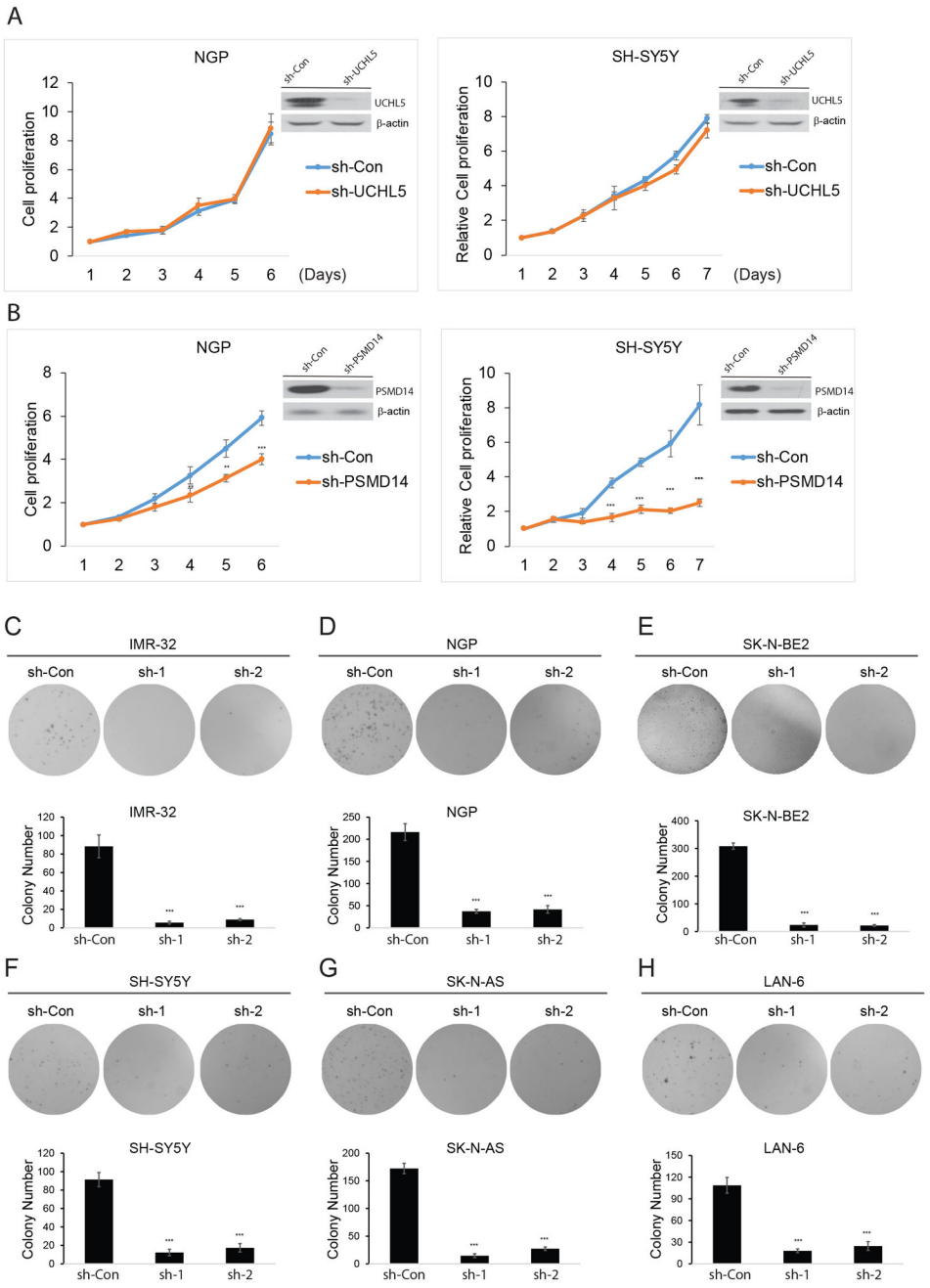

Figure 2: ***The effect of UCHL5 and PSMD14 knockdown on NB cell proliferation and USP14* knockdown inhibits anchorage-independent growth.**

A, B. Immunoblotting assay showing UCHL5 and PSM14 knockdown in NGP and SH-SY5Y cells by lentivirus sh-UCHL5 and sh-PSMD14. Cell growth curve assay shows a proliferation defect in two UCHL5 knockdown NB cells. The cell counting kit-8 (CCK-8) was used to determine cell viability. Error bars represent SDs of six samples. **P<0.01 and ***P<0.001. C-H. Soft agar assay showing reduced colony formation in *USP14*-knockdown cells. Colony numbers were quantified. These experiments were performed in triplicate and reported as mean with SDs. ****P*<0.001.

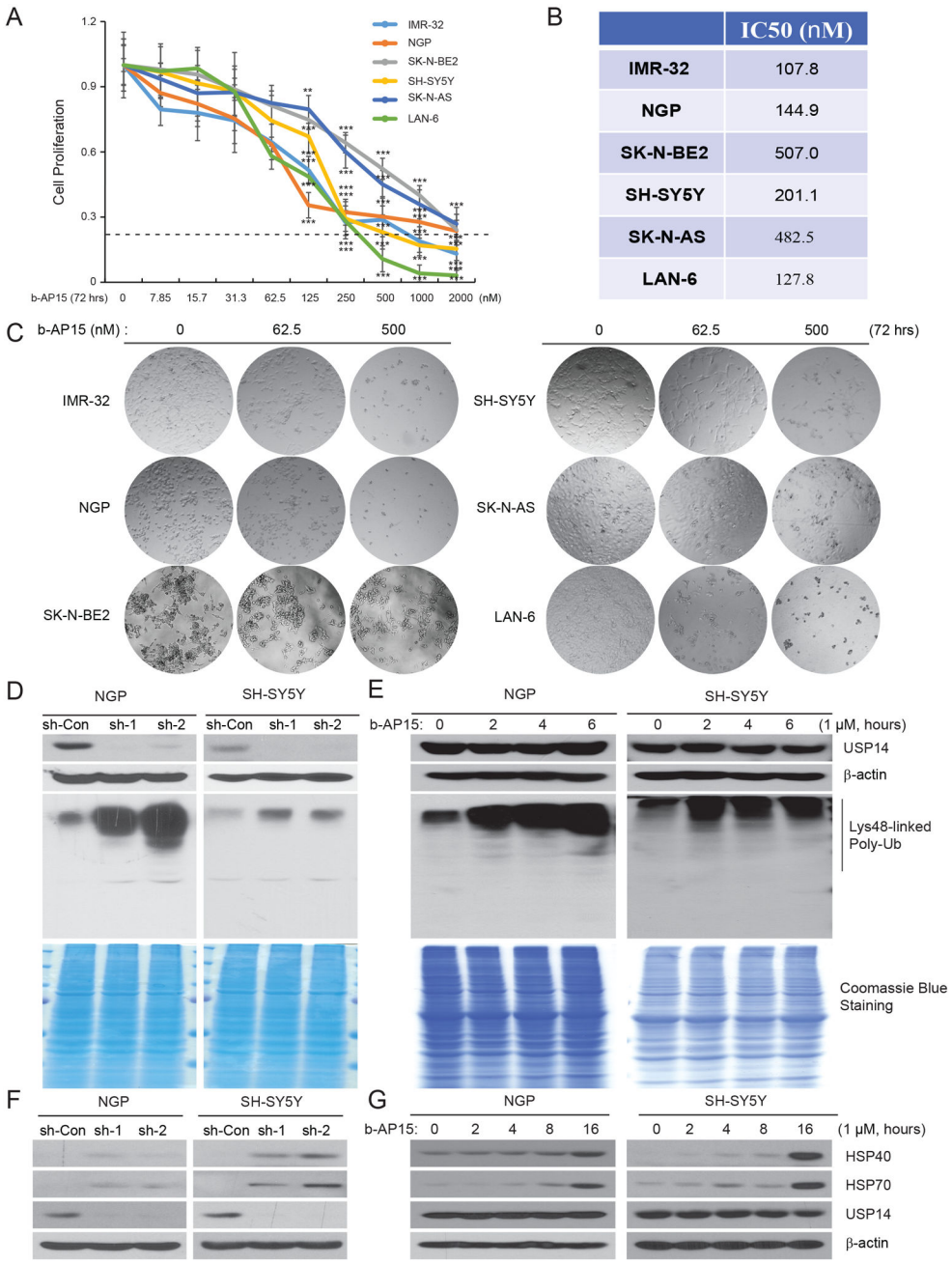

Figure 3: USP14 inhibitor b-AP15 suppresses cell proliferation, causes accumulation of ubiquitinated proteins and induces UPR in NB.

A. b-AP15 showing cytotoxic effect on NB cells. Six NB cell lines IMR-32, NGP, SK-N-BE2, SH-SY5Y, SK-N-AS, and LAN-6 were incubated with serial dilutions of b-AP15 or medium alone for 72 hours. Cell Counting Kit-8 (CCK-8) assay was used to determine cell viability. B. IC50 values of six cell lines tested were measured based on CCK-8 assay. C. Morphological changes of six NB cell lines after incubation with serial dilutions of b-AP15 for 72 hours were shown. D. Two *USP14*-knockdown cells, NGP and SH-SY5Y, were harvested, and subjected to immunoblotting with anti-Lys48-linked specific antibody. Same

amounts of lysates were performed Coomassie Blue staining as loading controls. E. NGP and SH-SY5Y cells were treated with b-AP15 (1 μM) for the indicated time points. Cell lysates were subjected to immunoblotting as the above. F, G. *USP14* knockdown NGP and SH-SY5Y (F) cells or b-AP15 treated NB cells (G) were subjected to immunoblotting with anti-HSP40, HSP70, and USP14 antibodies.

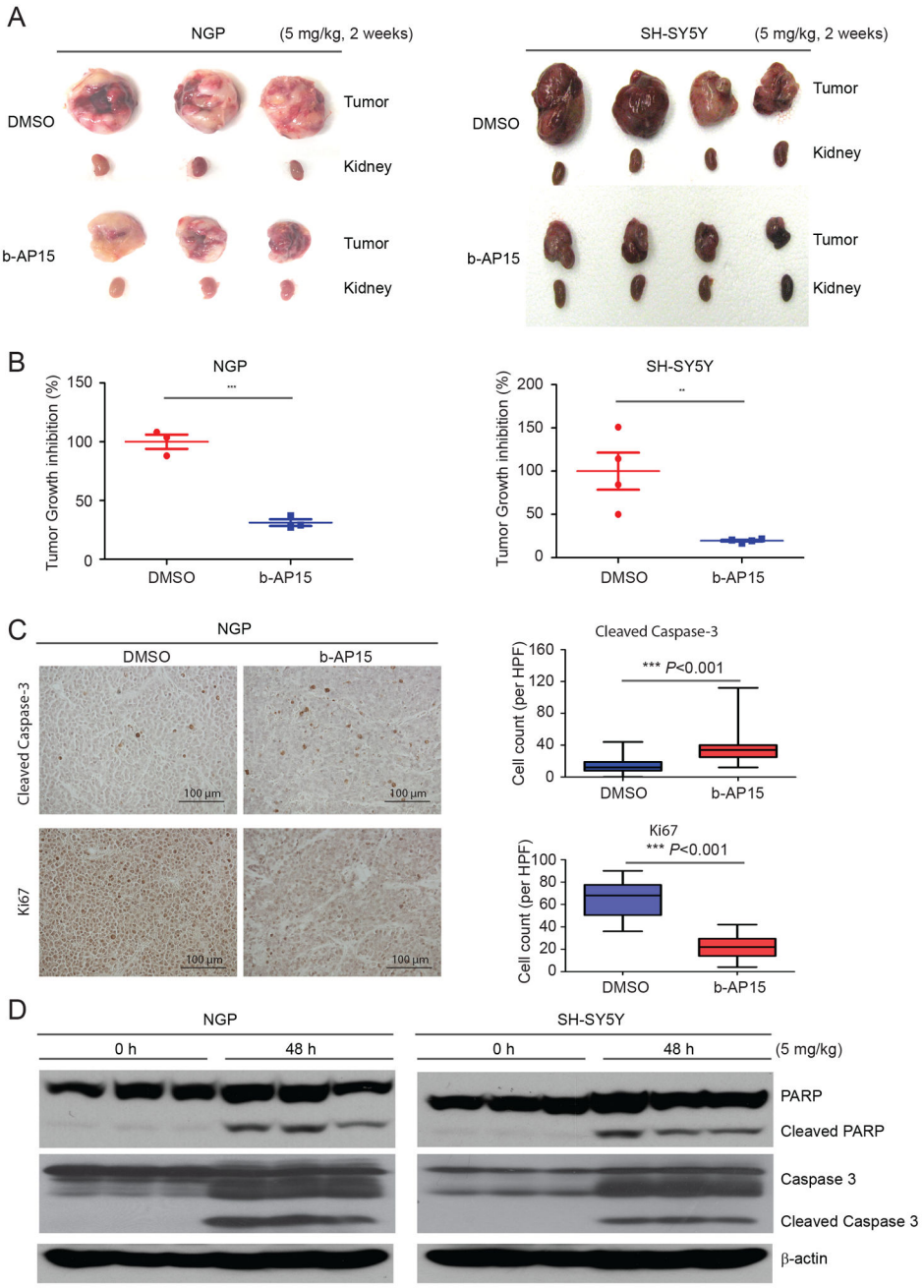

Figure 4: USP14 inhibitor b-AP15 suppresses NB tumor growth *in vivo*.

A. Representative pictures of orthotopic tumors in each group. The nude mice bearing tumors were treated with b-AP15 (5 mg/kg) and DMSO respectively for two weeks. B. Tumor weights from the last day of treatment. Data was from one experiment. ** P<0.01 and *** P<0.001. C. Representative light microscopy images of cleaved capspse-3 and Ki67 immunohistochemistry staining from NGP xenograft tumors treated with b-AP15 and DMSO control. Quantification of cleaved caspase-3 and Ki67 (positive cell per high-power field) demonstrates induction of apoptosis and inhibition of tumor growth in NGP xenografts treated with b-AP15. D. The nude mice bearing tumors were treated with 5 mg/kg of b-

AP15 by intraperitoneal injection once daily for two days. The mice were then euthanized, and immunoblotting assay was used to detect b-AP15-induced apoptosis.

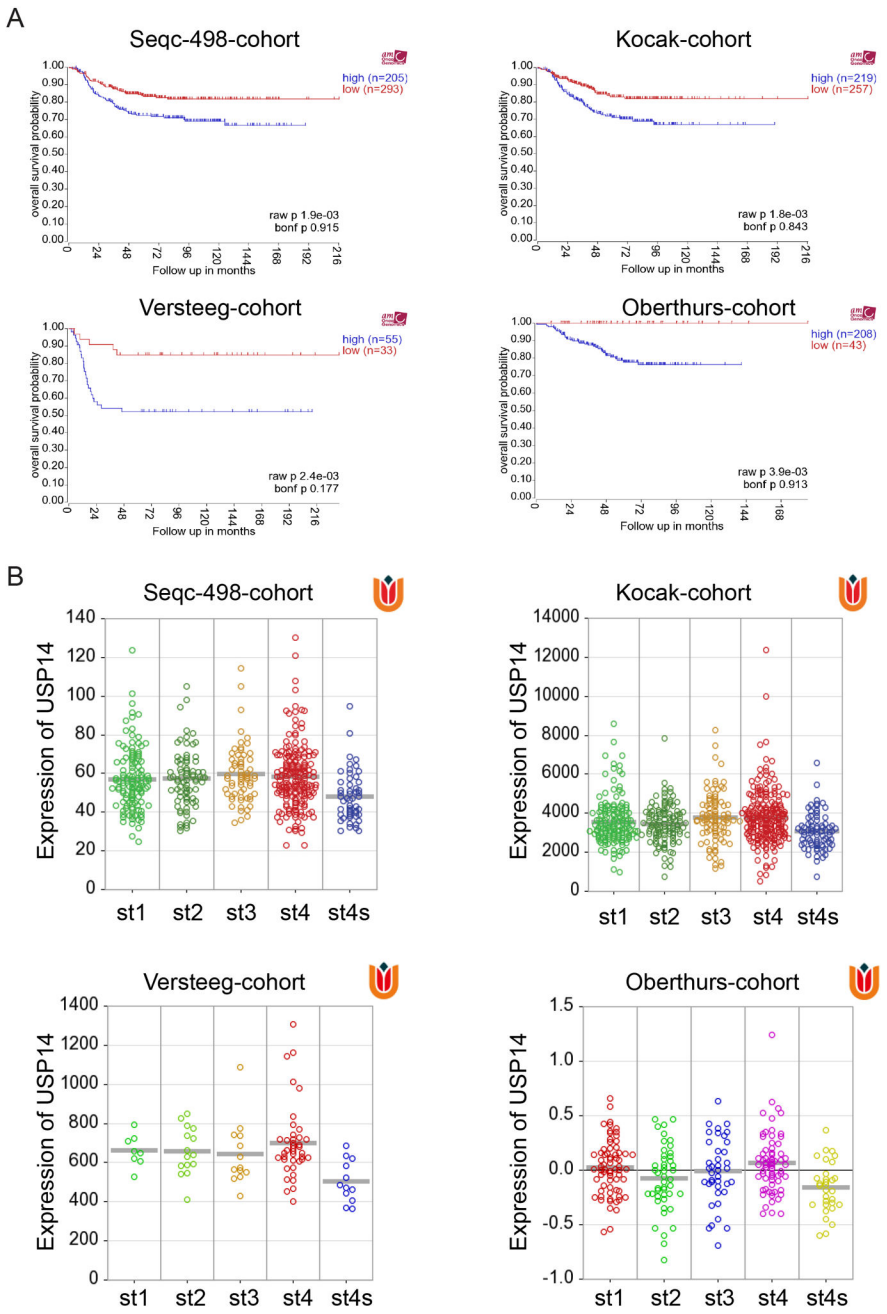

Figure 5. The mRNA level of *USP14* in NB patient samples.

A. Correlation of *USP14* mRNA levels of NB tumor samples and the overall survival of patients was analyzed using Seqc-498-cohort (n=498), Kocak-cohort (n=476), Versteeg-cohort (n=88), and Oberthurs-cohort (n=251). B. *USP14* mRNA levels in patient samples at different Stages were analyzed using these four datasets.

Table 1

Synergy analysis of b-AP15 with Doxorubicin or VP-16 in NB cells

		Combination Index (CI)		
Cell line		**ED50**	**ED75**	**ED90**
IMR-32	Doxorubicin+b-AP15	0.72	0.92	1.06
	VP-16+b-AP15	0.46	0.66	0.96
NGP	Doxorubicin+b-AP15	0.21	0.80	0.90
	VP-16+b-AP15	0.52	0.41	0.32
SK-N-BE2	Doxorubicin+b-AP15	0.96	0.63	0.48
	VP-16+b-AP15	0.31	0.47	0.81
SH-SY5Y	Doxorubicin+b-AP15	0.73	0.86	0.81
	VP-16+b-AP15	0.55	0.46	0.43
SK-N-AS	Doxorubicin+b-AP15	0.95	1.03	1.06
	VP-16+b-AP15	0.90	0.73	0.65
LAN-6	Doxorubicin+b-AP15	0.25	0.36	0.64
	VP-16+b-AP15	0.33	0.59	0.32

The combination index (CI) was assessed by CompuSyn software. CI < 1 indicates synergistic interaction, whereas CI > 1 is antagonistic and CI = 1 is considered additive effect. ED, Median effective dose.